MYCOSES

A *Candida auris*–specific adhesin, Scf1, governs surface association, colonization, and virulence

Darian J. Santana[1,2], Juliet A. E. Anku[1,3,4], Guolei Zhao[1], Robert Zarnowski[5,6], Chad J. Johnson[5,6], Haley Hautau[7], Noelle D. Visser[1]†, Ashraf S. Ibrahim[7,8], David Andes[5,6], Jeniel E. Nett[5,6], Shakti Singh[7,8], Teresa R. O'Meara[1]*

Candida auris is an emerging fungal pathogen responsible for health care–associated outbreaks that arise from persistent surface and skin colonization. We characterized the arsenal of adhesins used by *C. auris* and discovered an uncharacterized adhesin, Surface Colonization Factor (Scf1), and a conserved adhesin, Iff4109, that are essential for the colonization of inert surfaces and mammalian hosts. *SCF1* is apparently specific to *C. auris*, and its expression mediates adhesion to inert and biological surfaces across isolates from all five clades. Unlike canonical fungal adhesins, which function through hydrophobic interactions, Scf1 relies on exposed cationic residues for surface association. *SCF1* is required for *C. auris* biofilm formation, skin colonization, virulence in systemic infection, and colonization of inserted medical devices.

Since the initial reports of its discovery in 2009, the emerging fungal pathogen *Candida auris* has become an increasingly common source of life-threatening infection worldwide (*1*, *2*). *C. auris* is frequently reported in association with nosocomial outbreaks, a characteristic rarely described with other *Candida* species, and is of urgent concern for public health authorities (*3*–*7*). *C. auris* outbreaks are characterized by persistent colonization of patient skin and abiotic surfaces, which can remain positive for extensive periods and serve as a source of contaminative transmission (*8*–*14*). *C. auris* also colonizes indwelling medical devices, which act as a risk factor for the development of invasive disease (*15*–*21*). Lapses in diagnostic screening and infection prevention measures are thought to contribute to the increasing rate of *C. auris* outbreaks (*20*). The ability of *C. auris* to robustly colonize a range of living and abiotic substrates is central to its emergence as a global health threat.

Colonization requires the initial physical association and attachment between fungal cells and substrate. For fungal pathogens, attachment is largely mediated by cell surface–exposed adhesin proteins (*22*). In *Candida* species, genetic expansion has resulted in the formation of adhesin families containing genes similar in sequence and domain architecture, with adhesive functions that are redundant or specific across family members (*23*, *24*). *C. auris* encodes genes similar to members of the conserved *ALS (Agglutinin-Like Sequence)* and *IFF/HYR (IPF Family F/Hyphally Regulated)* adhesin families found across the genus, although these genes may have expanded independently in *C. auris* and lack clear one-to-one homology with adhesins from well-characterized species. Moreover, their phenotypic importance in *C. auris* is not well understood (*24*–*26*).

To investigate the role of individual *C. auris* adhesins in colonization phenotypes, we measured the adhesion between fungal cells and polymer substrates as a model for surface association. We found that *C. auris* does not primarily rely on conserved adhesins for surface attachment. Instead, we identified Surface Colonization Factor 1 (Scf1), an adhesin specific to *C. auris* that is necessary and sufficient for the robust attachment of its cells to polymer substrates. *C. auris* isolates from diverse and similar genetic lineages exhibit marked divergence in terms of substrate association, and this phenotypic plasticity is tightly correlated with strain-specific transcriptional control of *SCF1*. The nonspecific surface association driven by *Scf1* does not occur through canonical hydrophobic interactions but rather through cation-substrate interactions. To explore the clinical relevance of these findings, we investigated the importance of *SCF1* in long-term colonization models. *SCF1* is critical for biofilm formation in vitro, robust colonization of in vivo central venous catheters, colonization of both human and murine skin, and virulence in disseminated infection. These findings offer insight into the genetic and molecular mechanisms by which *C. auris* mediates surface association, a trait critical to the increasing disease burden of this emerging pathogen.

[1]Department of Microbiology and Immunology, University of Michigan, Ann Arbor, MI, USA. [2]Department of Epidemiology, University of Michigan, Ann Arbor, MI, USA. [3]West African Centre for Cell Biology of Infectious Pathogens (WACCBIP), Accra, Ghana. [4]Department of Biochemistry, Cell and Molecular Biology, University of Ghana, Accra, Ghana. [5]Department of Medicine, University of Wisconsin, Madison, WI, USA. [6]Department of Medical Microbiology and Immunology, University of Wisconsin, Madison, WI, USA. [7]Division of Infectious Disease, The Lundquist Institute for Biomedical Innovation at Harbor–University of California, Los Angeles Medical Center, Torrance, CA, USA. [8]David Geffen School of Medicine, University of California, Los Angeles, Los Angeles, CA, USA.
***Corresponding author. Email: tromeara@umich.edu**
†Present address: Department of Biology, University of Louisville, Louisville, KY, USA.

Results

Polymer surface attachment by the adhesin SCF1

C. auris encodes 12 genes homologous to members of the characterized *ALS* and *IFF/HYR* adhesin families (*24*, *25*, *27*). We generated individual deletion mutants in the clade I AR0382 background for each adhesin gene to model their impact on surface association. We used a flow cytometric adhesion assay that measures the ability of cells to attach to dispersed polystyrene microspheres in suspension (fig. S1) (*28*). Of the 12 adhesin mutants, only deletion of *IFF4109* (B9J08_004109) conferred an adhesive defect while still failing to completely ablate attachment (Fig. 1A). To investigate the possibility that there were occult adhesive factors, we screened a library of 2560 insertional mutants, prioritizing those exhibiting the most significant defects (Fig. 1B). The greatest loss of adhesive capacity was observed in the *tnSWI1* (B9J08_003460) and *tnBCY1* (B9J08_002818) mutants (Fig. 1, B and C, and fig. S2). Compared with the AR0382 parent, the *tnSWI1* mutant exhibited no significant transcriptional dysregulation of the *ALS* or *IFF/HYR* adhesins, suggesting alternative mediators of adhesion (Fig. 1D). The strongest, most significantly dysregulated gene in *tnSWI1* was an uncharacterized open reading frame (ORF) (B9J08_001458) that had no significant primary sequence homology to characterized genes (Fig. 1D). This gene, however, exhibited a putative three-domain architecture consistent with canonical glycosylphosphatidylinositol (GPI)–anchored fungal adhesins (Fig. 1E) (*23*). This same gene was also strongly down-regulated in the *tnBCY1* mutant, whereas *IFF4109* was not (fig. S2). Deletion of the B9J08_001458 ORF in AR0382 conferred a substantial adhesive defect, so we refer to the gene as *Surface Colonization Factor* (*SCF1*) (Fig. 1F). Complementation with an epitope-tagged *SCF1* allele in the endogenous locus rescued the adhesive defect, and the epitope-tagged Scf1 protein localized to the cell surface, consistent with its role as an adhesin (Fig. 1, F and G). Deletion of *IFF4109* in the Δ*scf1* background did not significantly reduce attachment beyond deletion of *SCF1* alone, suggesting nonadditive oles for these adhesins (Fig. 1F).

The specific reliance on Scf1 and Iff4109 for adhesion despite potential redundancy with other adhesins is reminiscent of other fungal pathogens. For instance, loss of *ALS1* alone reduces *Candida albicans* adhesion despite the presence of seven other *ALS* genes (fig. S3A) (*29*). In *C. auris*, adhesins exhibit structural and transcriptional variation, which may explain their functional specificity (fig. S3B) (*25*, *26*). However, *IFF4892* encodes the entire canonical adhesin architecture and shows similar expression to *IFF4109*, but of the two, only *IFF4109* is required for adhesion, suggesting

that individual adhesins mediate specific adhesive mechanisms (Fig. 1A and fig. S3B) (*25*). Such functional specificity is shown by the increased flocculation and aggregation associated with overexpression of *ALS4112*, whereas these phenotypes are not associated with *SCF1* despite its transcriptional expression being among the highest 2.5% of all genes in this strain background (fig. S3, B to D) (*30*, *31*). These findings suggest functional specificity for surface association for Scf1 and Iff4109.

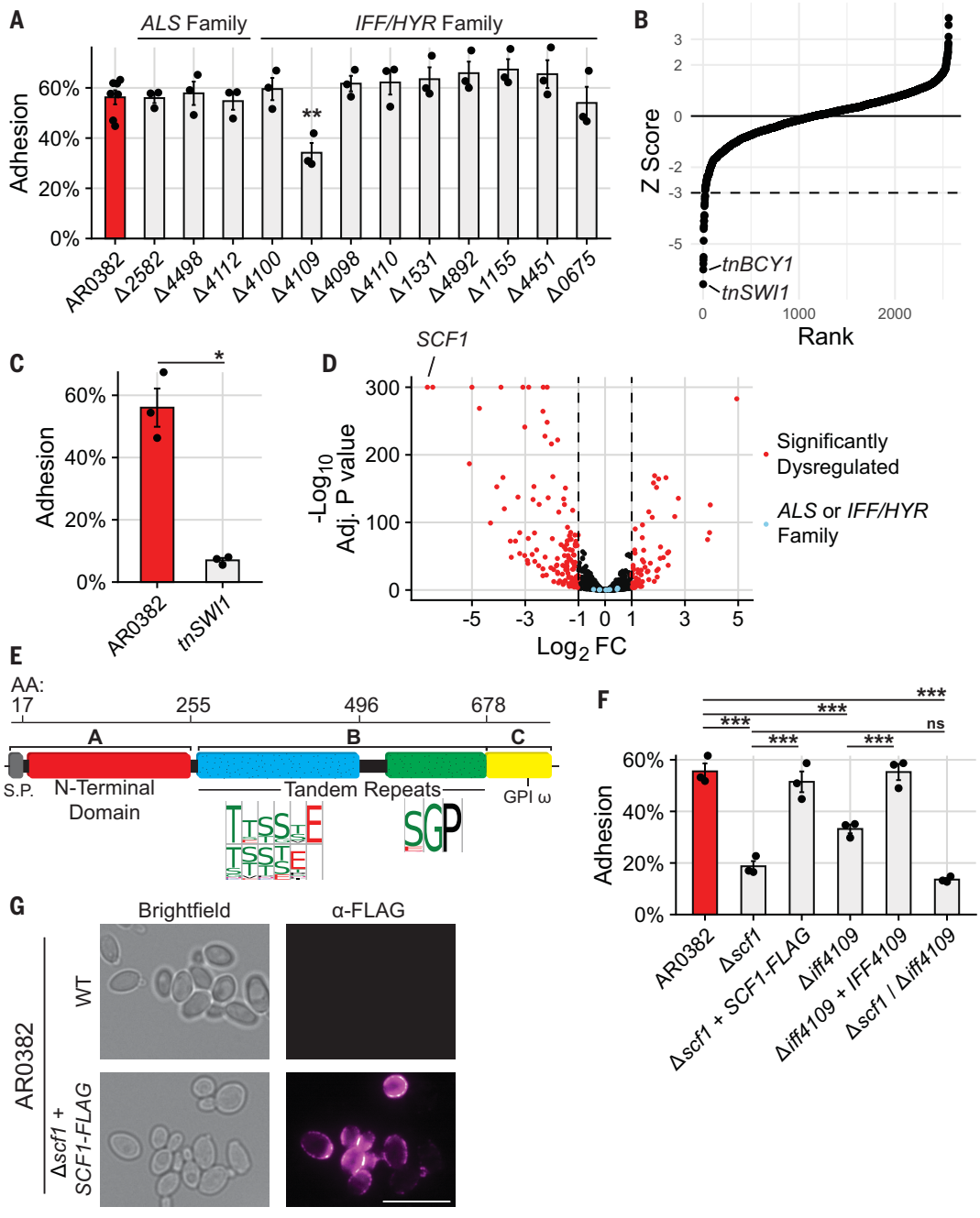

Fig. 1. SCF1 mediates *C. auris* adhesion to polymer surfaces. (**A**) Adhesion of wild-type AR0382 or mutants lacking one of 12 genes from the *ALS* or *IFF/HYR* adhesin families. (**B**) The 2560 insertional mutants in the AR0382 strain background were screened for adhesion defects by measuring the proportion of cells able to remain attached to a cyclic olefin polymer surface after three washes with phosphate-buffered saline. Strains are ordered by *Z*-score rank. Mutants with a *Z*-score more negative than −3 were considered to have a significant adhesive defect. (**C**) Adhesion of AR0382 and an insertional *SWI1* mutant. (**D**) RNA sequencing comparing the transcriptome of *tnSWI1* with that of AR0382. *SCF1* (B9J08_001458) is the strongest dysregulated gene. (**E**) Predicted domain architecture of Scf1 based on the clade I primary sequence is consistent with canonical fungal adhesins. (**F**) Adhesion of adhesin mutants and complements compared with AR0382. (**G**) Immunofluorescence microscopy using an α-FLAG antibody. Representative images shown for wild-type AR0382 and AR0382 Δ*scf1* + *SCF1-FLAG*. Scale bar, 5 μm. Statistical differences were assessed using one-way ANOVA with Dunnett's post hoc test (A), Student's *t* test (C), or one-way ANOVA with Tukey's post hoc test (F); $*P \le 0.05$; $**P \le 0.01$; $***P \le 0.001$; ns: $P > 0.05$.

C. auris relies on Scf1 for adhesive plasticity

Although many *Candida* and *Saccharomyces* adhesins belong to conserved gene families, we identified homologs of *SCF1* only in *C. auris* and the closely related *Candida haemulonii* species and not in other members of the *haemulonii* complex (Fig. 2A). *SCF1* is encoded in a genomic locus in *C. auris* and *C. haemulonii* that is syntenic, lacking an *SCF1* homolog, even to distantly related species (Fig. 2A). Although the *C. haemulonii SCF1* homolog functionally complements Δ*scf1* in *C. auris,* it is not essential for adhesion in *C. haemulonii* and shows poor expression across isolates, indicating that reliance on *SCF1* for adhesion is specific to *C. auris* (fig. S4).

To investigate the generalizability of the reliance on *SCF1* and the variability between *C. auris* strains, we measured adhesion for 23 *C. auris* isolates representing all five clades and diverse geographic origins. These strains exhibited substantial adhesive variation regardless of clade ($P = 2 \times 10^{-16}$, $F = 35.06$, one-way ANOVA) (Fig. 2B). By contrast, a similar analysis of 19 genetically diverse *C. albicans* clinical isolates showed no significant adhesive variation ($P = 0.054$, $F = 1.856$, one-way ANOVA), indicating that the surface association strategies of *C. auris* are more plastic than those of *C. albicans* (Fig. 2C). Substantial variation in adhesion was observed even between genetically similar isolates of *C. auris*, e.g., AR0382 and AR0387, which differ by only 206 coding single-nucleotide polymorphisms (Fig. 2B). In the poorly adhesive AR0387, *SCF1* was the most down-regulated gene compared with the highly adhesive AR0382, reminiscent of the poorly adhesive *tnSWI1* mutant (fig. S5A and Fig. 1D). However, the transcriptome of AR0387 showed little overlap with that of the *tnSWI1* strain, indicating that dysregulation of *SCF1* in AR0387 is not caused by a *SWI/SNF* complex defect (fig. S5B). Furthermore, we observed no nucleotide variants in the *SCF1* ORF or neighboring intragenic regions between AR0382 and AR0387.

Transcript abundance of *SCF1* was tightly positively correlated with adhesion across isolates regardless of clade ($r = 0.87$, $P = 8.4 \times 10^{-8}$) (Fig. 2D). By contrast, we observed no association between transcriptional control of *IFF4109* and adhesion ($r = 0.3$, $P = 0.25$) (Fig. 2D). Experimentally, transcriptional overexpression of *SCF1* was sufficient to elevate adhesion in the otherwise poorly adhesive isolate AR0387 (Fig. 2E). The magnitude of overexpression using the *TEF1* promoter (~2^8-fold increase) was similar to and did not exceed the naturally varying magnitude of expression difference between the two wild-type isolates AR0382 and AR0387 (~2^9-fold change) (Fig. 2, D and E). These data show that adhesive variation between *C. auris* isolates is associated with *SCF1* expression variation.

In AR0382 and AR0387, the *SCF1* locus is invariant, but other isolates exhibit allelic variation, which is primarily concentrated in the low-complexity tandem repeats (table S1). We tested whether allelic variation also contributed to the adhesive variation among isolates. Overexpression of the native *SCF1* allele in AR0381, a poorly adhesive clade II isolate, was sufficient to increase attachment (fig. S6A). However, overexpression of the clade I *SCF1* allele from AR0382 further elevated adhesion despite similar levels of overexpression (fig. S6A). In the clade I AR0382 background, which relies strongly on *SCF1* for adhesion, complementation of the Δ*scf1* mutant with either the clade I or clade II *SCF1* allele resulted in

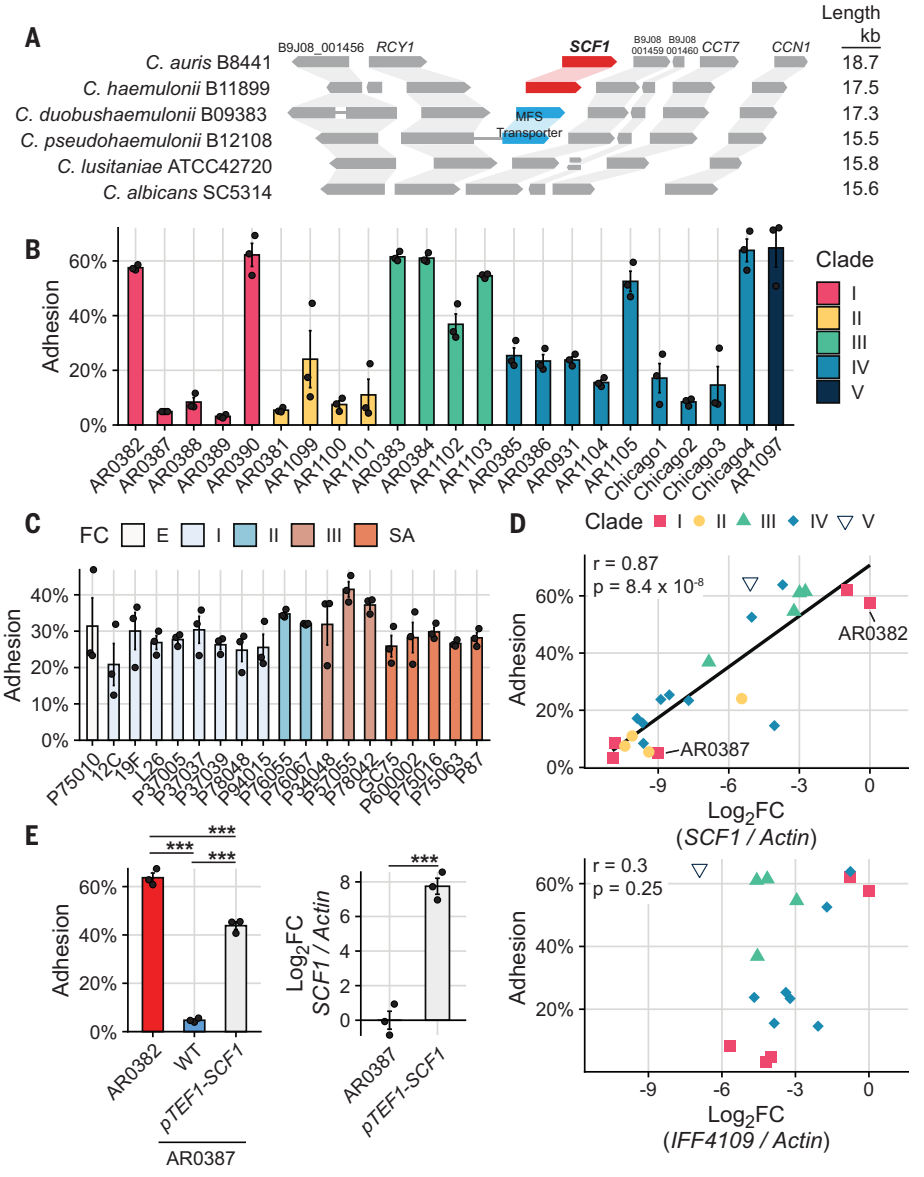

Fig. 2. *C. auris* alone relies on Scf1 for adhesive plasticity. (**A**) Synteny schema depicting *SCF1* and the conservation and orientation of adjacent ORFs. Genomic loci are shown compared with *C. auris*. Putative *SCF1* homologs were only identified in *C. auris* and *C. haemulonii*. (**B**) Adhesion of 23 *C. auris* clinical isolates from all five clades. (**C**) Adhesion of 19 *C. albicans* clinical isolates from five clades. FC, fingerprint clade. (**D**) *SCF1* transcript abundance (top panel), but not *IFF4109* transcript abundance (bottom panel), is associated with adhesion to polystyrene in the same 23 *C. auris* isolates from (A). Log_2 fold change (Log_2FC) values are expressed relative to AR0382. Each point signifies the mean of three biological replicates. Pearson correlation coefficient and *P* value are indicated. Isolates that do not encode *IFF4109* are not indicated in the bottom panel. (**E**) Comparison of adhesion between two clade I isolates: AR0382 and AR0387. Overexpression of *SCF1* using the strong *TEF1* promoter (right panel) is sufficient to drive adhesion in the poorly adhesive AR0387 background (left panel). Statistical differences were assessed using one-way ANOVA [(B) and (C)], Tukey's post hoc test (E), or Student's *t* test (E); *$P \leq 0.05$; **$P \leq 0.01$; ***$P \leq 0.001$; ns: $P > 0.05$.

similar levels of rescue of the adhesive phenotype (fig. S6B). These findings show that sequence variation between these two *SCF1* alleles does not intrinsically contribute to functional differences in adhesion, and that other factors may also influence adhesive capacity.

Scf1 *and* Iff4109 *have distinct nonspecific mechanisms*

The reliance on *SCF1* for surface association is complicated by the genetic interaction with *IFF4109*, in which deletion of both does not result in a more severe adhesive defect than deletion of *SCF1* alone (Fig. 1F). Loss of one adhesin did not result in dysregulation of the other, suggesting that the interaction is not a regulatory one (fig. S7). One possibility is that the two genes contribute to adhesion through distinct but complementary physical mechanisms. For other *Candida* species, adhesion to abiotic substrates is often nonspecific, with adhesins promoting affinity for hydrophobic substrates (*32*–*34*). The highly adhesive AR0382 strain exhibited elevated cell surface hydrophobicity compared with the poorly adhesive AR0387 (Fig. 3, A and B). Deletion of the *IFF4109* adhesin in AR0382 reduced cell surface hydrophobicity, which was rescued to wild-type levels by complementation (Fig. 3, A and B). By contrast, deletion or overexpression of *SCF1* did not significantly affect cell surface hydrophobicity in either AR0382 or AR0387 (Fig. 3, A and B).

Elevated cell surface hydrophobicity likewise promotes affinity for hydrophobic substrates (*33*). We measured the adhesion of *C. auris* isolates to both an untreated hydrophobic polystyrene surface and a polystyrene surface modified using vacuum plasma treatment to become strongly hydrophilic. Both Iff4109 and Scf1 mediated adhesion to the hydrophobic substrate (Fig. 3C); however, only Scf1 mediated adhesion to the hydrophilic substrate, showing that Scf1 is not dependent on hydrophobicity (Fig. 3D). AR0382 and AR0387 still exhibited differential adhesion to the hydrophilic surface, indicating that hydrophobic interactions are not primarily responsible for the differential strain phenotypes (Fig. 3D).

To investigate the mechanism of Scf1 adhesion, we examined the apical N-terminal domain using AlphaFold2, which suggested that this domain contains a core fibronectin type III fold similar to the *FLO11* family of adhesins characterized in *Saccharomyces cerevisiae* and conserved throughout *Ascomycota* (fig. S8A) (*32*, *35*). However, Scf1 does not exhibit significant primary sequence homology to *S. cerevisiae* Flo11 and lacks conservation of the canonical aromatic bands responsible for adhesive functions in true *FLO11* homologs (fig. S8, A and B) (*32*, *35*). Furthermore, model confidence dwindles outside of the fibronectin fold, suggesting substantial variation from Flo11

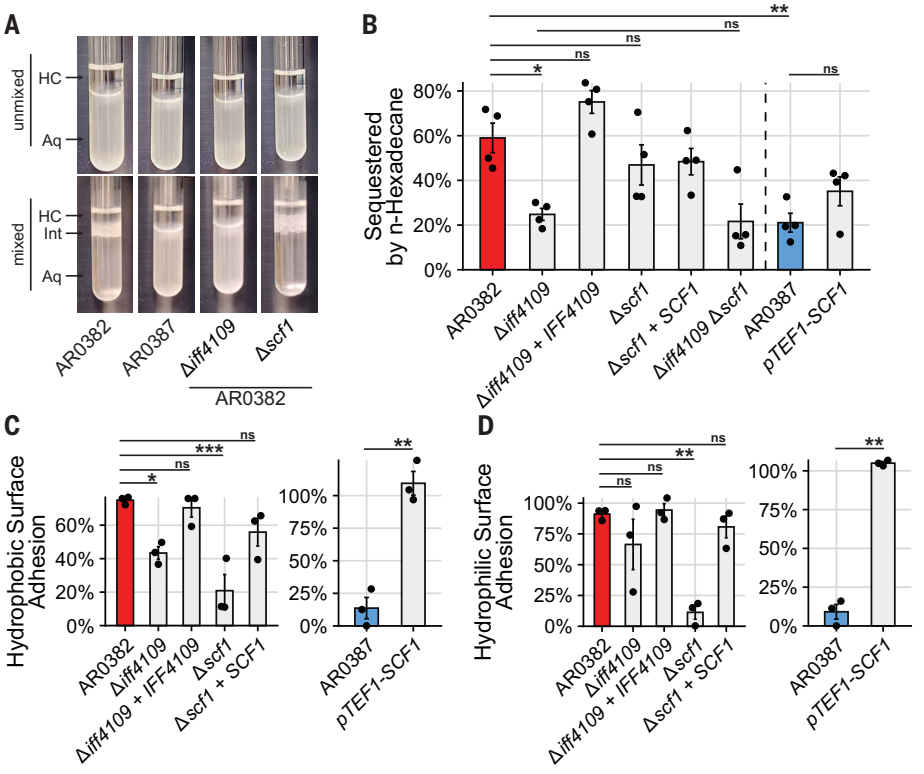

Fig. 3. Iff4109, but not Scf1, mediates adhesion through cell surface hydrophobicity. (**A**) Representative images from the microbial attachment to hydrocarbons (MATH) assay. Hydrophobic cells are sequestered from the aqueous phase (Aq) to the aqueous-hydrocarbon interface (Int) after mixing with the hydrocarbon phase (HC). (**B**) Proportion of cells sequestered out of the aqueous phase during the MATH assay. (**C** and **D**) Cells were allowed to attach to a hydrophobic, untreated polystyrene surface (C) or a hydrophilic, vacuum plasma–treated polystyrene surface (D) for 1 hour. The surface was then washed and the proportion of cells that remained attached after washing was measured. Statistical differences were assessed using one-way ANOVA with Tukey's post hoc test [(B), (C), and (D)] or Student's *t* test [(C) and (D)]; $*P \leq 0.05$; $**P \leq 0.01$; $***P \leq 0.001$; ns: $P > 0.05$.

adhesins (fig. S9). In its primary sequence, the Scf1 N-terminal domain exhibits an enrichment of arginine and lysine residues compared with other yeast adhesins (table S2). Adhesive systems in many marine organisms rely on similarly cation-rich proteins, which act through the displacement of hydrated ions at the surface-liquid interface or direct cation-π interactions with substrates (*36*–*40*). We reasoned that if Scf1 relied on such interactions, then adhesion could be inhibited by a saturating concentration of cations at the substrate interface that could not be competitively displaced by SCF1. Consistent with this hypothesis, high concentrations of arginine in solution were sufficient to ablate AR0382 adhesion (Fig. 4A). Similar concentrations of NaCl or other noncationic amino acids did not produce the same effect, whereas exogenous lysine produced a more modest inhibition of attachment, consistent with lysine's weaker ability to form electrostatic interactions (Fig. 4B) (*41*).

We next investigated whether specific cationic regions or residues were critical for Scf1 activity. We generated point mutations in cationic residues in different areas of the N-terminal domain, focusing on residues that clustered with aromatic groups because this pattern potentiates electrostatic adhesion (fig. S10A) (*42*). Several mutations had no adhesive impact, but an R54A R55A mutant exhibited a modest adhesive defect while showing no discernable effect on Scf1 transcription, protein expression, or localization (fig. S10). Mutating the entire cation-aromatic cluster, H52 H53 R54 R55, resulted in a similar adhesive defect (Fig. 4, C and D, and fig. S11). A nearby cation-aromatic cluster, K44-K49, which was modeled to be less surface exposed, was not required for adhesion (Fig. 4, C and D, and fig. S11). To determine whether surface exposure of the HHRR cluster (residues 52 to 55) would be sufficient to promote adhesion, we synthesized peptides corresponding to Scf1 residues 50 to 62 with the intact wild-type cluster or the HHRR residues mutated. The wild-type peptide adhered to polystyrene microspheres, but mutation of the HHRR cluster completely ablated this ability

(Fig. 4, E and F). Similar patterns of cation-aromatic clusters are also abundant in some lipid-binding proteins (*40*, *43*). The wild-type Scf1 peptide was similarly able to adhere to phosphotidylcholine microparticles, and *SCF1* expression potentiated lipid particle binding by *C. auris* cells, suggesting that Scf1 may also contribute to association with biotic substrates (fig. S12).

SCF1 promotes long-term colonization and virulence

We next investigated the impact of Scf1 and Iff4109 on other aspects of surface colonization. We measured the importance of these adhesins for biofilm growth, which can promote prolonged environmental persistence (*11*, *44*–*46*). The two adhesins were functionally redundant, and deletion of both was required to ablate biofilm formation in AR0382, suggesting that the partial adhesive contributions of each is sufficient to establish colonization (fig. S13A). Expression of *SCF1* alone in otherwise biofilm-incompetent isolates was sufficient to establish biofilm colonization (fig. S13, B to E). This pattern continued for in vivo biofilms, in which loss of *SCF1* and *IFF4109* ablated the ability of AR0382 to colonize the luminal surface of a polyethylene rat central venous catheter, and overexpression of *SCF1* was sufficient to potentiate AR0387 colonization (Fig. 5, A and B).

We then investigated whether biological surface association followed the same reliance on these adhesins. Again, we observed that loss of *SCF1* and *IFF4109* diminished the ability of AR0382 to colonize ex vivo human skin explants and in vivo murine skin, whereas overexpression of *SCF1* potentiated skin colonization by AR0387 (Fig. 5, C and D, and fig. S14). Given this potential for interaction with host tissues, we also investigated the importance of these adhesins in disseminated infection. Histopathological examination of tissues collected from immune-compromised mice 7 days after intravenous *C. auris* infection revealed that the loss of *SCF1* and *IFF4109* reduced AR0382 dissemination to the kidneys and heart, whereas overexpression of *SCF1* in AR0387 was sufficient to increase fungal lesions (Fig. 5, E and F, and fig. S15). Loss of *SCF1* and *IFF4109* substantially attenuated the virulence of AR0382, with the wild type causing 100% mortality within 12 days of infection and the mutant causing 20% mortality after 21 days (Fig. 5G). Similarly, overexpression of *SCF1* reduced the median survival time of mice infected with AR0387 from 18.5 to 11.5 days and ablated the difference in overall survival between the less virulent AR0387 and the more virulent AR0382 (Fig. 5G).

Discussion

C. auris encodes genes similar to the conserved *ALS* and *IFF/HYR* adhesin families, and proposed models suggest that differential utilization of these adhesins may contribute to epidemiological

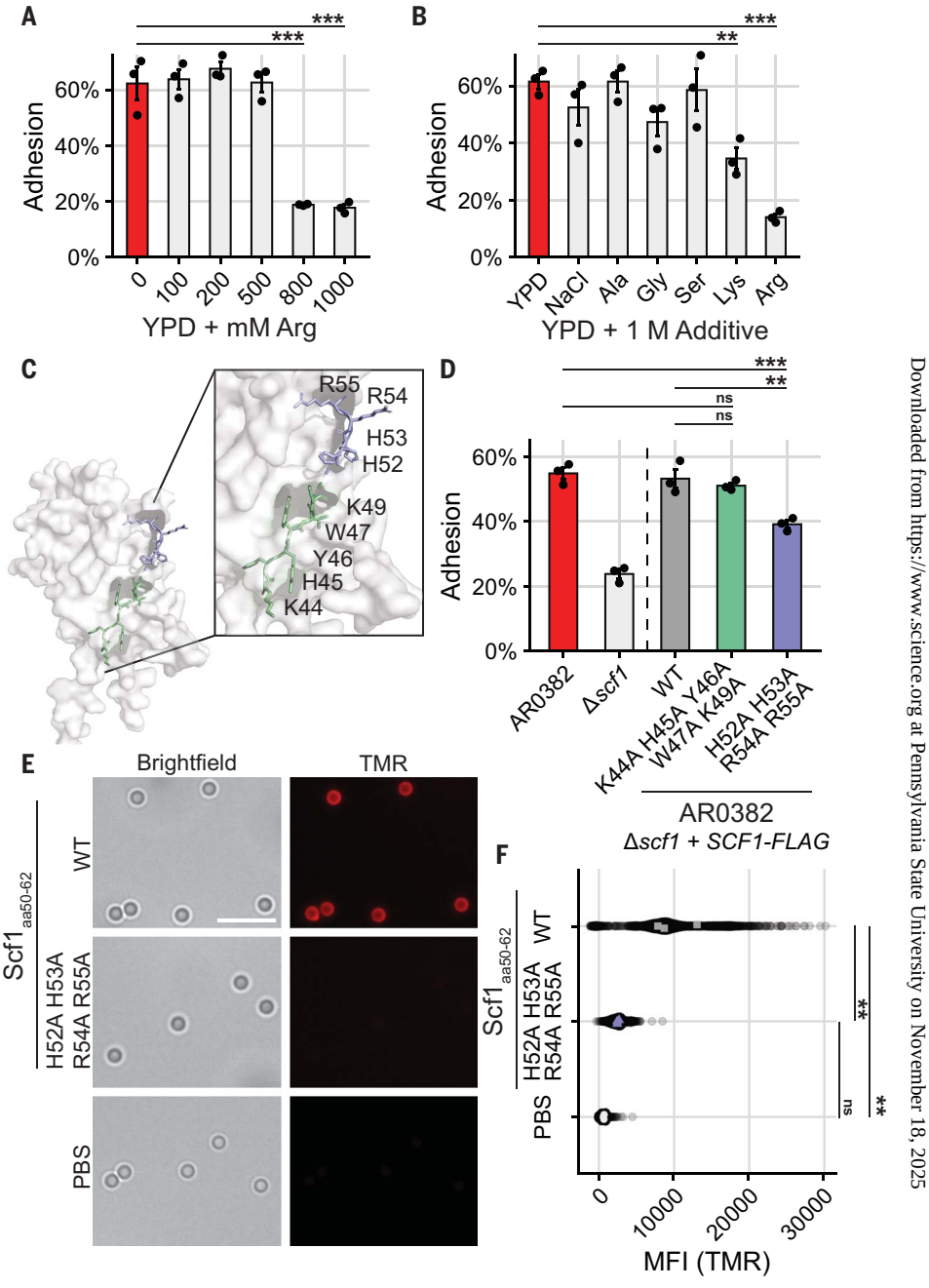

Fig. 4. Specific cationic residues are critical for Scf1-mediated surface association. (**A** and **B**) Wild-type AR0382 adhesion in the presence of increasing concentrations of arginine (A) or 1 M additives (B). (**C**) Predictive model of the Scf1 N-terminal domain with two neighboring cationic-aromatic clusters highlighted. (**D**) Adhesion of wild-type AR0382, a mutant lacking *SCF1*, or AR0382 Δ*scf1* + *SCF1-FLAG* mutants encoding the wild-type *SCF1* allele or alleles containing the indicated mutations. (**E**) Tetramethylrhodamine (TMR)–labeled 13–amino acid peptides corresponding to the wild-type Scf1 sequence (residues 50 to 62) or the same sequence with the indicated mutations incubated with the same polystyrene microspheres used to measure adhesion in (D). Scale bar, 5 μm. (**F**) Quantification (mean fluorescence intensity, MFI) of peptide binding to individual polystyrene microspheres as in (E) measured by TMR epifluorescence and corrected for background fluorescence. Each point represents an individual microsphere. Colored points represent averages of individual experiments used for statistical analysis. Statistical differences were assessed using one-way ANOVA with Dunnett's post hoc test [(A) and (B)] or one-way ANOVA with Tukey's post hoc test [(D) and (F)]; $^{*}P \le 0.05$; $^{**}P \le 0.01$; $^{***}P \le 0.001$; ns: $P > 0.05$.

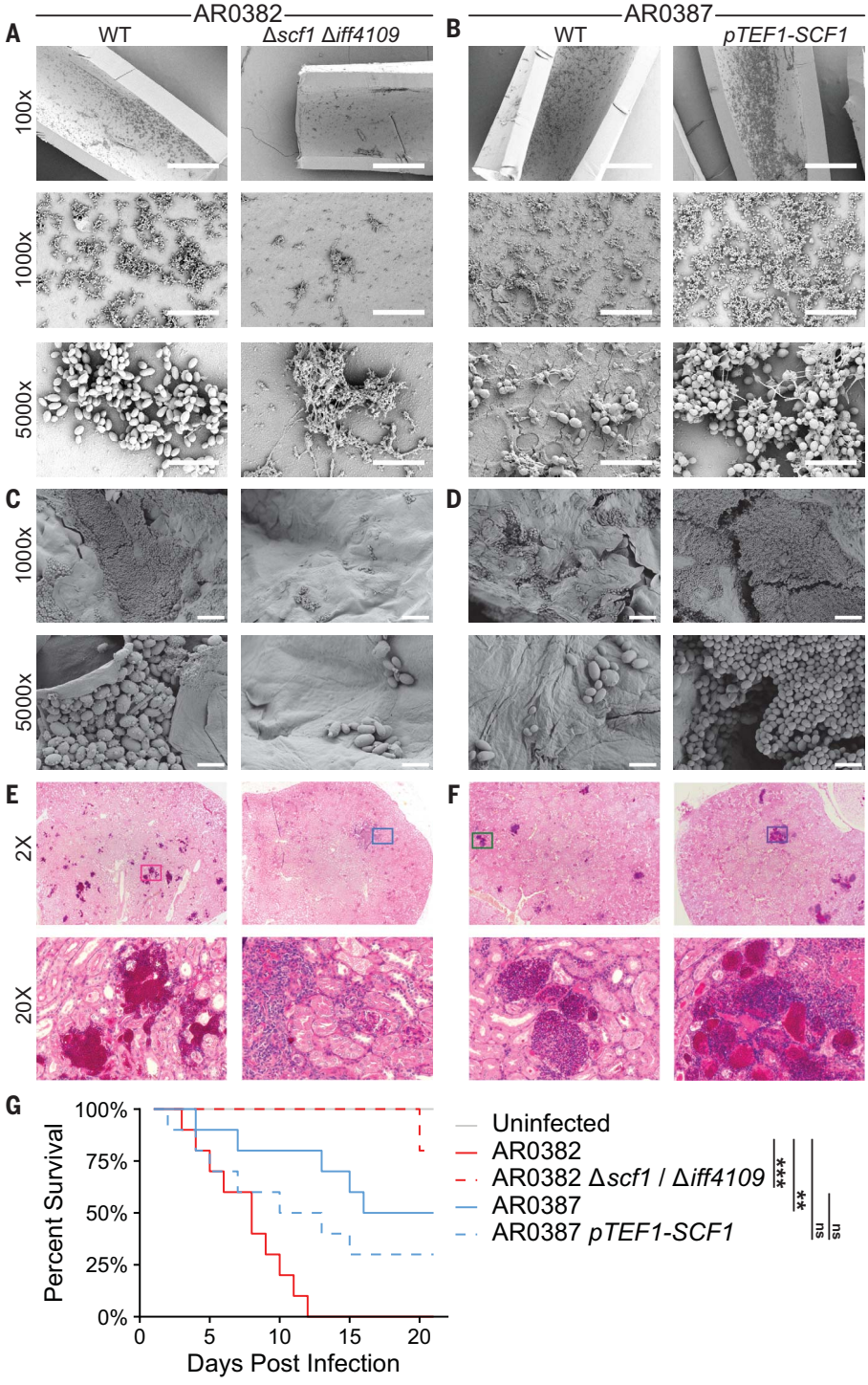

Fig. 5. Scf1 mediates host colonization and infection phenotypes. (**A** and **B**) Polyethylene central venous catheters were set in rat jugular veins and inoculated intraluminally with *C. auris*. Representative scanning electron microscopy images of the luminal catheter surface are shown from catheters collected 24 hours after infection. Scale bars: 400 μm (100×), 40 μm (1000×), and 5 μm (5000×). (**C** and **D**) Full thickness human skin explants were colonized with *C. auris* for 24 hours before washing to remove unassociated cells. Representative scanning electron microscopy images of the skin surface after washing are shown. Scale bars: 20 μm (1000×) and 4 μm (5000×). (**E** to **G**) Immunosuppressed mice were infected intravenously (through tail vein injection) with 5×10^7 *C. auris* cells. Histopathology sections of the kidneys 7 days after infection [(E) and (F)] were stained with periodic acid–Schiff. Magenta color indicates lesion areas. Ten infected mice for each strain were monitored for survival for 21 days (G). Statistical comparisons of overall survival were assessed using the Mantel-Haenszel log-rank test with Benjamini-Hochberg correction; *$P \leq 0.05$; **$P \leq 0.01$; ***$P \leq 0.001$; ns $P > 0.05$.

differences among isolates (*25*, *27*). Our findings suggest that the *C. auris*–specific adhesin Scf1 and the conserved adhesin Iff4109 are the principal mediators of association with abiotic surfaces and additionally contribute substantially to infection and long-term colonization of both biological and abiotic surfaces. The other conserved adhesin genes did not appear to mediate surface association. Whether this is the product of functional or regulatory divergence remains to be explored. We observed widespread differential regulation of *SCF1* among *C. auris* isolates regardless of clade, suggesting that the transcriptional control of this adhesin has adapted more recently than clade separation. The widespread plasticity around a single genetic element responsible for diverse, clinically relevant phenotypes could be problematic in outbreak settings. Although Scf1 and Iff4109 contribute to host infection and colonization, the mechanisms of their interaction with host systems remain unclear. Understanding how variable adhesion allows *C. auris* to mediate infection is likely to offer therapeutic insights. Prior work suggests that vaccination or monoclonal antibody therapy targeting Als or Iff/Hyr adhesins may offer protection against lethal *C. auris* infection (*27*, *47*). Furthermore, the complementary function of Scf1 and Iff4109 with divergent mechanisms suggests that *C. auris* has evolved the capacity for promiscuous surface association and colonization. Mediation of hydrophobic interactions is largely conserved among fungal adhesins, consistent with the adhesive mechanism of the conserved Iff4109 (*32*–*34*). The cation-rich Scf1, however, appears to functionally resemble proteins from bivalve, barnacle, and *Vibrio* adhesion systems. For these organisms, cation-dependent surface interactions promote adhesion in aqueous and highly ionic environments (*36*–*39*). *C. auris* has been isolated from the coastal wetlands of the Andaman Islands and from a Colombian estuary, suggesting a possible marine natural habitat, and this ecological niche may have conferred similar selective pressures on adhesion mechanisms (*48*, *49*). Development of this specific adhesion biology may in part explain the tenacity of this organism on medically relevant substrates. Nevertheless, differential utilization of *SCF1* by different isolates suggests that an unknown selective pressure may govern its expression. Understanding this adaptation and its clinical consequences more fully may offer important insights into the outbreak potential of this pathogen.

Overall, our work characterizes of the adhesin machinery used by *C. auris* for surface association and colonization. The identification of Scf1 and the characterization of the genetic determinants of adhesion add to the growing understanding of the pathobiology of this emerging organism.

REFERENCES AND NOTES

1. A. Chakrabarti, P. Sood, *J. Med. Microbiol.* **70**, 001318 (2021).
2. A. B. Akinbobola, R. Kean, S. M. A. Hanifi, R. S. Quilliam, *PLOS Pathog.* **19**, e1011268 (2023).
3. L. Ashkenazi-Hoffnung, C. Rosenberg Danziger, *J. Fungi (Basel)* **9**, 176 (2023).
4. N. A. Chow *et al*., *Lancet Infect. Dis.* **18**, 1377–1384 (2018).
5. S. C. Roberts, T. R. Zembower, E. A. Ozer, C. Qi, *J. Clin. Microbiol.* **59**, e02252-20 (2021).
6. S. Vallabhaneni *et al*., *MMWR Morb. Mortal. Wkly. Rep.* **65**, 1234–1237 (2016).
7. World Health Organization, "WHO fungal priority pathogens list to guide research, development and public health action" (WHO, 2022); https://www.who.int/publications/i/item/9789240060241).
8. D. J. Sexton *et al*., *Clin. Infect. Dis.* **73**, 1142–1148 (2021).
9. D. M. Proctor *et al*., *Nat. Med.* **27**, 1401–1409 (2021).
10. E. Adams *et al*., *Emerg. Infect. Dis.* **24**, 1816–1824 (2018).
11. O. Dire, A. Ahmad, S. Duze, M. Patel, *J. Hosp. Infect.* **137**, 17–23 (2023).
12. J. N. de Almeida Jr *et al*., *Mycoses* **64**, 1062–1072 (2021).
13. D. W. Eyre *et al*., *N. Engl. J. Med.* **379**, 1322–1331 (2018).
14. C. A. Patterson *et al*., *Crit. Care Med.* **49**, 697–701 (2021).
15. T. Vila *et al*., *MSphere* **5**, e00760-20 (2020).
16. K. Vinayagamoorthy, K. C. Pentapati, H. Prakash, *Mycoses* **65**, 613–624 (2022).
17. E. Rajni, A. Jain, S. Gupta, Y. Jangid, R. Vohra, *Acta Med. (Hradec Kralove)* **65**, 83–88 (2022).
18. J. V. Mulet Bayona, N. Tormo Palop, C. Salvador García, M. D. R. Guna Serrano, C. Gimeno Cardona, *Mycoses* **66**, 882–890 (2023).
19. F. Allaw *et al*., *Microorganisms* **10**, 1011 (2022).
20. M. Lyman *et al*., *Ann. Intern. Med.* **176**, 489–495 (2023).
21. K. Benedict, K. Forsberg, J. A. W. Gold, J. Baggs, M. Lyman, *Emerg. Infect. Dis.* **29**, 1485–1487 (2023).
22. P. W. J. de Groot, O. Bader, A. D. de Boer, M. Weig, N. Chauhan, *Eukaryot. Cell* **12**, 470–481 (2013).
23. L.-O. Essen, M. S. Vogt, H.-U. Mösch, *Biol. Chem.* **401**, 1389–1405 (2020).
24. R. A. Smoak, L. F. Snyder, J. S. Fassler, B. Z. He, *Genetics* **223**, iyad024 (2023).
25. J. F. Muñoz *et al*., *Genetics* **218**, iyab029 (2021).
26. S.-H. Oh *et al*., *Front. Cell. Infect. Microbiol.* **11**, 794529 (2021).
27. S. Singh *et al*., *PLOS Pathog.* **15**, e1007460 (2019).
28. A. Silva-Dias *et al*., *Cytometry A* **81**, 265–270 (2012).
29. J. S. Finkel *et al*., *PLOS Pathog.* **8**, e1002525 (2012).
30. C. Pelletier, A. J. P. Brown, A. Lorenz, *bioRxiv* p. 2023.04.21.537817 (2023).
31. J. Bing *et al*., *PLOS Pathog.* **19**, e1011239 (2023).
32. T. Kraushaar *et al*., *Structure* **23**, 1005–1017 (2015).
33. S. El-Kirat-Chatel *et al*., *ACS Nano* **9**, 1648–1655 (2015).
34. C. Valotteau, V. Prystopiuk, B. P. Cormack, Y. F. Dufrêne, *MSphere* **4**, e00277-19 (2019).
35. S. Brückner *et al*., *eLife* **9**, e55587 (2020).
36. G. P. Maier, M. V. Rapp, J. H. Waite, J. N. Israelachvili, A. Butler, *Science* **349**, 628–632 (2015).
37. Y. Li *et al*., *Mater. Chem. Front.* **1**, 2664–2668 (2017).
38. C. Liang *et al*., *Front. Mar. Sci.* **6**, 565 (2019).
39. S. Kim *et al*., *ACS Nano* **11**, 6764–6772 (2017).
40. X. Huang *et al*., *Nat. Commun.* **14**, 2104 (2023).
41. S. Sokalingam, G. Raghunathan, N. Soundrarajan, S.-G. Lee, *PLOS ONE* **7**, e40410 (2012).
42. H. Fan *et al*., *Nat. Commun.* **10**, 5127 (2019).
43. S. McLaughlin, J. Wang, A. Gambhir, D. Murray, *Annu. Rev. Biophys. Biomol. Struct.* **31**, 151–175 (2002).
44. R. Kean *et al*., *Int. J. Antimicrob. Agents* **52**, 673–677 (2018).
45. R. Kean *et al*., *MSphere* **3**, e00334-18 (2018).
46. B. Short *et al*., *J. Hosp. Infect.* **103**, 92–96 (2019).
47. S. Singh *et al*., *J. Fungi (Basel)* **9**, 103 (2023).
48. P. Arora *et al*., *mBio* **12**, e03181-20 (2021).
49. P. Escandón, *J. Fungi (Basel)* **8**, 748 (2022).

ACKNOWLEDGMENTS

We thank J. Sexton (University of Michigan) for consultation on the development of a label-free high-throughput imaging-based adhesion assay, M. Siddiq (University of Michigan) for consultation in investigating *SCF1* homology and variants, and A. Abraham (University of Michigan) for consultation on surface modification and assistance with vacuum plasma treatment experiments. **Funding:** This work was supported by the National Institutes of Health (grant R21AI169186 to D.J.S. and T.R.O.; grants T32AI007528 and F31AI169823 to D.J.S.; grant T32AI007413 to G.Z.; grant R01AI073289 to D.A.; grants R01AI145939 and R21AI159583 to J.E.N.; UCLA CTSI grant KL2TR001882 to S.S., and grant R01AI141202 to A.S.I.); the American Heart Association (grant 938451 to S.S.); and the WACCBIP (World Bank ACE Masters Fellowship and WACCBIP-NCDs Awandare to J.A.E.A.).

Author contributions: Conceptualization: D.J.S., T.R.O.; Funding acquisition: D.J.S., D.A., J.E.N., S.S., A.S.I., T.R.O.; Investigation: D.J.S., J.A.E.A., G.Z., R.Z., C.J.J., H.H., N.D.V., S.S.; Methodology: D.J.S., J.A.E.A., G.Z., R.Z., C.J.J., A.S.I., D.A., J.E.N., S.S., T.R.O.; Project administration: D.J.S., T.R.O.; Supervision: T.R.O., D.A., J.E.N., S.S., A.S.I.; Visualization: D.J.S., R.Z., C.J.J., S.S.; Writing – original draft: D.J.S., T.R.O., S.S., C.J.J., R.Z., J.A.E.A., G.Z.; Writing – review and editing: D.J.S., J.A.E.A., G.Z., R.Z., C.J.J., H.H., N.D.V., A.S.I., D.A., J.E.N., S.S., T.R.O. **Competing interests:** T.R.O. and D.J.S. are inventors on US Provisional Patent 63/502,704 filed on 17 May 2023 and US Provisional Patent 63/514,470 filed on 19 July 2023 related to this work. The remaining authors declare no competing interests. **Data and materials availability:** Data from Illumina sequences are available in the National Center for Biotechnology Information Sequence Read Archive (NCBI SRA; https://www.ncbi.nlm.nih.gov/sra/) under BioProject accession number PRJNA904261 (for RNA-sequencing data) or PRJNA904262 (for *Agrobacterium tumefaciens*–mediated transformation mutant whole-genome sequencing). Strains and constructs generated in this study will be provided for research purposes upon request. All remaining data are available in the main text or the supplementary materials. **License information:**

SUPPLEMENTARY MATERIALS

science.org/doi/10.1126/science.adf8972
Materials and Methods
Figs. S1 to S15
Tables S1 to S5
References (*50*–*77*)
Data S1
MDAR Reproducibility Checklist

Submitted 5 December 2022; resubmitted 2 July 2023
Accepted 23 August 2023
10.1126/science.adf8972